Tetrahedron: *Asymmetry* xxx (2015) xxx–xxx

Contents lists available at ScienceDirect

Tetrahedron: *Asymmetry*

journal homepage: www.elsevier.com/locate/tetasy

Resolutions of sibutramine with enantiopure tartaric acid derivatives: chiral discrimination mechanism

Yu Hu [a,*], Jia-jie Yuan [a], Xiao-xia Sun [b], Xi-mei Liu [b], Zhen-hong Wei [a], Xun Tuo [a], Hui Guo [a]

[a] *Department of Chemistry and Education Center for Basic Chemistry Experiments, Nanchang University, Nanchang 330031, China*
[b] *Jiangxi Key Laboratory of Functional Organic Molecules, Jiangxi Normal University of Science & Technology, Nanchang 330013, China*

ARTICLE INFO

Article history:
Received 13 January 2015
Revised 1 April 2015
Accepted 5 April 2015
Available online xxxx

ABSTRACT

The resolution of sibutramine **1** was investigated with enantiopure tartaric acid derivatives. Based on the resolving efficiency assay using a 'Dutch resolution', *O*,*O*′-di-*p*-anisoyl-(*R*,*R*)-tartaric acid (*R*,*R*)-DMTA was identified as an effective resolving agent, which is easily obtained from natural and inexpensive (*R*,*R*)-tartaric acid. Compound (*R*)-**1** was obtained with high enantiomeric purity and yield. The chiral discrimination mechanism and resolving effect in the process were explained with X-ray crystallographic studies. The crystal structures of the conglomerate salts revealed that the more soluble diastereomer (*S*)-**1**·(*R*,*R*)-DMTA formed a parallel ribbon supramolecular structure while the less soluble diastereomer (*R*)-**1**·(*R*,*R*)-DMTA formed a spiral net packing structure by enantio-differentiation self-assembly. The effect of the side substituent of the resolving agent on the enantioseparation of **1** via a supramolecular chiral host consisting of tartaric acid analogues is discussed.

1. Introduction

Approximately half of all commercial drugs are chiral. Many racemic medicines have been researched and upgraded in the domain of chiral preparation and application. Sibutramine **1**, as an anti-obesity drug, is a serotonin and noradrenaline re-uptake inhibitor. It has been proven to be effective in weight reduction.[1] The stereogenic carbon atom of sibutramine has two enantiomeric isomers. Its enantioselective behaviors have been revealed in the pharmacokinetic and pharmacodynamic characteristics.[2,3] Compound (*R*)-**1** decreases body weight and food uptake, whereas the (*S*)-isomer increases body weight and food uptake.[4,5] Animal experiments show that (*R*)-**1** can reduce dosage and lower side effects.[6] Meanwhile, it has been found that (*R*)-**1** can potentially be used in the treatment of depression, Parkinson's disease, cerebral function disorders and diabetes.[7] For efficiency and safety, sibutramine should be developed and administered as a single isomer drug. Although asymmetric synthesis is one way to obtain (*R*)-**1**,[8] it is unsuitable for commercial production. Alternatively, the racemate has some well-established preparation methods and is manufactured on a large scale. Therefore, the resolution of the racemate via diastereomeric intermediates is a reasonable method for the commercial synthesis of chiral sibutramine.

Tartaric acid and its derivatives are well known to be good resolving agents for racemic amines. The *rac*-**1** was first resolved with *O*,*O*′-dibenzoyl-tartaric acid (DBTA),[9] and enantiomerically pure **1** was prepared with >99.5% enantiomeric excess in 40% overall yield. However, (*R*)-**1** was obtained only by (*S*,*S*)-DBTA, which is not as abundant as natural (*R*,*R*)-tartaric acid. Herein, we explored the resolution with (*R*,*R*)-tartaric acid derivatives for the first time. A very efficient method was reported for the resolution of *rac*-**1**. *O*,*O*′-Di-*p*-anisoyl-(*R*,*R*)-tartaric acid (*R*,*R*)-DMTA **4** was found to be the best resolving agent among (*R*,*R*)-DBTA **2**, *O*,*O*′-di-(*p*-toluoyl)-(*R*,*R*)-tartaric acid (*R*,*R*)-DTTA **3** and **4** (Scheme 1).

Classical resolution depends on the different solubility of diastereomeric salt pairs, which is the result of the molecular interactions of the corresponding diastereomeric salt.[10] Over the past two decades, the crystal structures of paired diastereomeric salts were investigated to clarify the mechanism of chiral discrimination.[11–15] Few studies have probed the crystal structures of the resolving salts with 'Dutch resolution' to gain insights into chiral recognition mechanism.[16] Herein, the effect of the side substituent of the resolving agent on the enantioseparation of **1** is discussed. The crystal structures of the less-soluble salts were compared in using DBTA and DMTA. To elucidate chiral discrimination, we studied the crystal structures of paired diastereomeric salts of chiral sibutramine with **4** by X-ray crystallographic analysis. We investigated the supramolecular structure of these resolving salts and the relationships between structure and molecular

* Corresponding author. Tel.: +86 791 83969494.
E-mail address: huyu@ncu.edu.cn (Y. Hu).

http://dx.doi.org/10.1016/j.tetasy.2015.04.007
0957-4166/

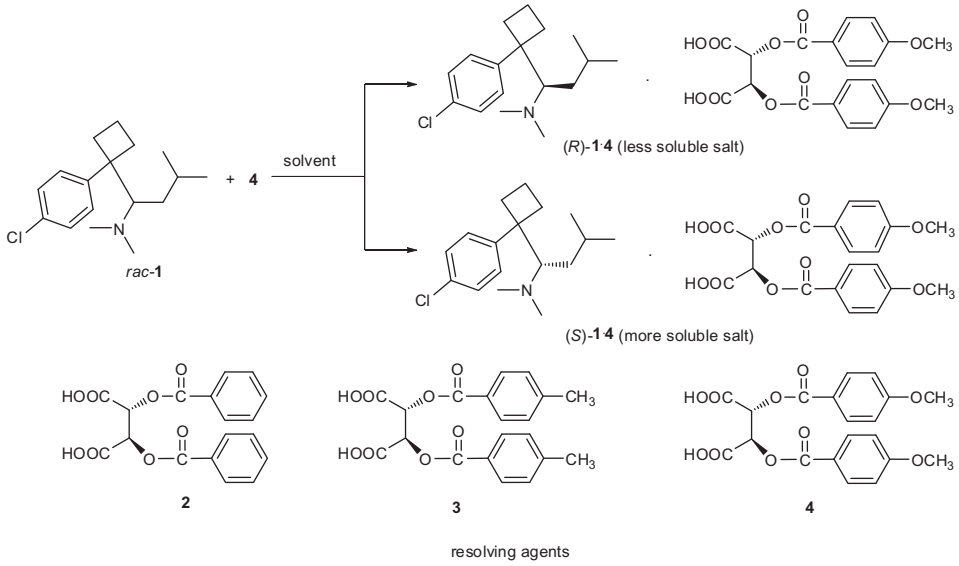

Scheme 1. Resolution of racemic **1**.

recognition to understand why the resolving efficiency of **4** is the best for the resolution of **1**.

2. Results and discussion

2.1. Resolution of sibutramine

Tartaric acid and its diaryl carboxylate derivatives **2**, **3,** and **4** are among the most widely used chiral acids for the resolution of racemic amines,[17] such as DBTA for racemic sibutramine **1**.[9] To improve the resolution efficiency, the three compounds were explored with diastereomeric salts. At first, we explored a mixed group of **2**, **3,** and **4** as the resolving agent. The mixture of resolving agents was added to a solution of equimolar amounts of *rac*-**1** in ethyl acetate, and the precipitate was analyzed by ^{1}H NMR and HPLC. Compound (*R*)-**1** was obtained with 43.4% yield and 62.3% enantiomeric excess (Table 1, entry 1). According to ^{1}H NMR results, Dutch resolution of *rac*-**1** was carried out with a mixture of **2**, **3,** and **4**. After recrystallization of the salt, **4** became the major component in the complex, in which the molar ratio of **2**, **3,** and **4** changed from 3:7:20 to 2:11:50 (Table 1, entries 1 and 2). When the mixture of **3** and **4** was used with equimolar *rac*-**1**, the resolving efficiency increased to 38.2% (Table 1, entry 3). Meanwhile, the resolution was carried out with **3** or **4** alone. The salt of **1**·**3** was difficult to precipitate out and the resolving efficiency of **4** was better than others (Table 1, entry 4). These demonstrated that **4** was the best resolving agent. Compound (*R*)-**1** could be obtained with up to 75.3% efficiency with **4**.

Furthermore, several solvents, such as methanol, ethanol, isopropanol, acetone, and dichloromethane were studied, and the mixed solvent of ethanol and *n*-hexane was found to be an excellent solvent system. In the resolution with tartaric acid derivatives, the usual molar ratio of racemic amine and resolving agent was 1:1. To improve the resolving efficiency of **4**, we tested several ratios between host and guest during the resolution of *rac*-**1**. Optimization experiments showed that the ratio of 0.9:1 was the best (Table 1, entries 5–11). In the experiments, ^{1}H NMR demonstrated that the ratios of **4** and **1** in the less-soluble salts were close to 1:1. After recrystallization in isopropyl alcohol, the less soluble diastereomer (*R*)-**1**·(*R*,*R*)-DMTA was treated with alkali to release (*R*)-**1** with >98% enantiomeric excess. Thus, utilizing **4** as a resolving agent, enantiomerically pure (*R*)-**1** was prepared with 98.6%

Table 1
Results of resolution of *rac*-**1**

Entry	**1**:**2**:**3**:**4**[a]	Solvent	ee[b] (%)	Yield[c] (%)	Eff.[d] (%)
1	3:1:1:1	Ethyl acetate	62.3	43.4	27.0 (3:7:20)[e]
2	—[f]	Ethyl acetate	83.1	58.2	— (2:11:50)[e]
3	4:0:1:3	Ethyl acetate	77.5	49.3	38.2
4	1:0:0:1	Ethyl acetate	78.7	95.6	75.3
5	1:0:0:1	Ethanol/*n*-hexane	82.8	95.9	79.4
6	1:0:0:0.9	Ethanol/*n*-hexane	89.4	91.3	81.6
7	—[g]	Isopropanol	98.6	92.5	—
8	1:0:0:0.8	Ethanol/*n*-hexane	88.5	88.0	77.9
9	1:0:0:0.7	Ethanol/*n*-hexane	87.9	80.4	70.7
10	1:0:0:0.6	Ethanol/*n*-hexane	89.1	74.7	66.6
11	1:0:0:0.5	Ethanol/*n*-hexane	91.4	68.9	63.0

[a] Initial molar ratio of *rac*-**1**, **2**, **3** and **4**.
[b] In all experiments, (*R*)-**1** was obtained and the enantiomeric purity was determined by HPLC.
[c] Yield of (*R*)-**1** based on half the initial amount of *rac*-**1**.
[d] Resolving efficiency, defined as a product of the yield of the diastereomeric salt and the ee of the liberated **1**.
[e] Molar ratio of **2**, **3** and **4** in the precipitated salts.
[f] Recrystallization from the mixed salt of entry 1.
[g] Recrystallization from the salt of entry 6.

Please cite this article in press as: Hu, Y.; et al. *Tetrahedron: Asymmetry* (2015), http://dx.doi.org/10.1016/j.tetasy.2015.04.007

Table 2
Crystallographic data collection and structural refinement information

	The more-soluble salt **5**	The less-soluble salt **6**
Configuration	(*S*)-**1**·**4**	(*R*)-**1**·**4**
Z	2	4
Crystal system	Monoclinic	Orthorhombic
Crystal size (mm)	0.30 × 0.25 × 0.12	0.40 × 0.30 × 0.25
Space group	*P* 2(1)	*P* 2(1) 2(1) 2(1)
a (Å)	7.972(3)	12.6906(11)
b (Å)	10.367(3)	14.6766(13)
c (Å)	22.220(7)	19.2061(18)
α (°)	90.00	90.00
β (°)	98.388(5)	90.00
γ (°)	90.00	90.00
Volume (Å^3)	98.388(5)	3577.2(6)
Wavelength (Å)	0.71073	0.71073
F(000)	740	3577.2(6)
Δ(*ρ*)max, min (e Å^{-3})	0.9808, 0.9529	0.9599, 0.9369

enantiomeric excess, with a yield of 84.5%; a typical resolution procedure is described in Section 4.

2.2. Crystal structures of diastereomeric salts

The supramolecular arrangement and packing of organic molecules in a crystal structure depend on numerous intermolecular interactions.[18] In chemical resolution via diastereomeric salt formation, host and guest molecules recognize each other by various interactions on the basis of their molecular structures and functional groups. To explore the chiral recognition ability of **4**, the more soluble diastereomeric salt (*S*)-**1**·(*R*,*R*)-DMTA was prepared by combining equimolar amounts of (*S*)-**1** and **4** in ethyl acetate. ^{1}H NMR showed that the more-soluble salt consists of (*S*)-**1** and **4** in a ratio of 1:1. Single crystals of more-soluble salt (*S*)-**1**·(*R*,*R*)-DMTA **5** and less-soluble salt (*R*)-**1**·(*R*,*R*)-DMTA **6** were obtained from ethanol. The crystallographic data of the crystals **5** and **6** are summarized in Table 2.

It is interesting to note that both diastereomeric salts form ordered supramolecular assemblies via hydrogen bonded networks. The more-soluble salt (*S*)-**1**·(*R*,*R*)-DMTA forms a parallel ribbon supramolecular structure (Fig. 1A and B), while crystal **6** prepared from the less-soluble salt (*R*)-**1**·(*R*,*R*)-DMTA shows a spiral net supramolecular motif (Fig. 2A and B). Notably, some main characteristics of the supramolecular structures are similar in the paired diastereomeric salts. In both supramolecules, two carboxylate groups of DMTA point to opposite directions (Figs. 1C and 2C). In crystals **5** and **6**, the ammonium ion of sibutramine holds one DMTA molecule by salt-bridge hydrogen bonds in the parallel supramolecule host-chains (Figs. 1B and 2B).

In fact, the difference of the paired diastereomeric salts **5** and **6** is due to their supramolecular structures. In crystal **5**, (*S*)-**1** and (*R*,*R*)-DMTA constitute the parallel ribbon supramolecule. (*R*,*R*)-DMTA molecules are interlinked by hydrogen bonds formed by the carboxylate groups of the two neighboring DMTA, and self-assemble to ribbon chain structure (Fig. 1C). DMTA molecules rank repeatedly as the same configuration along the axis and form zipper motif. The length of one host-unit along the *a* axis is 7.97 Å. The interactions of DMTA substituents, π–π stacking effect, and hydrogen bonds, make two neighboring closed zippers. The molecules of sibutramine present on two sides of the zip-closed by salt bridge bonds, and each zip-closed structure forms a ribbon chain (Fig. 1B).

In crystal **6**, a net supramolecule is constructed by (*R*)-**1** and (*R*,*R*)-DMTA via compact hydrogen bonded networks. In the supramolecular structure, (*R*,*R*)-DMTA molecules are interlinked via hydrogen bonded networks to form the spiral net structure (Fig. 2A and B). The intermolecular hydrogen bonds formed between the two neighboring DMTA molecules along the *a* axis is the same as that of **5** (Figs. 1C and 2C), and pack the DMTA molecules as a helix along the axis in crystal **6**. The skeletal structure exists as a 2_{14}-helix. The pitch of the helix is 12.69 Å. In the helical chain, the four methoxybenzoyl substituents of the two neighboring DMTA direct to different directions. It shows a spiral fishbone motif (Fig. 2C). The parallel adjacent screw chains arrange in

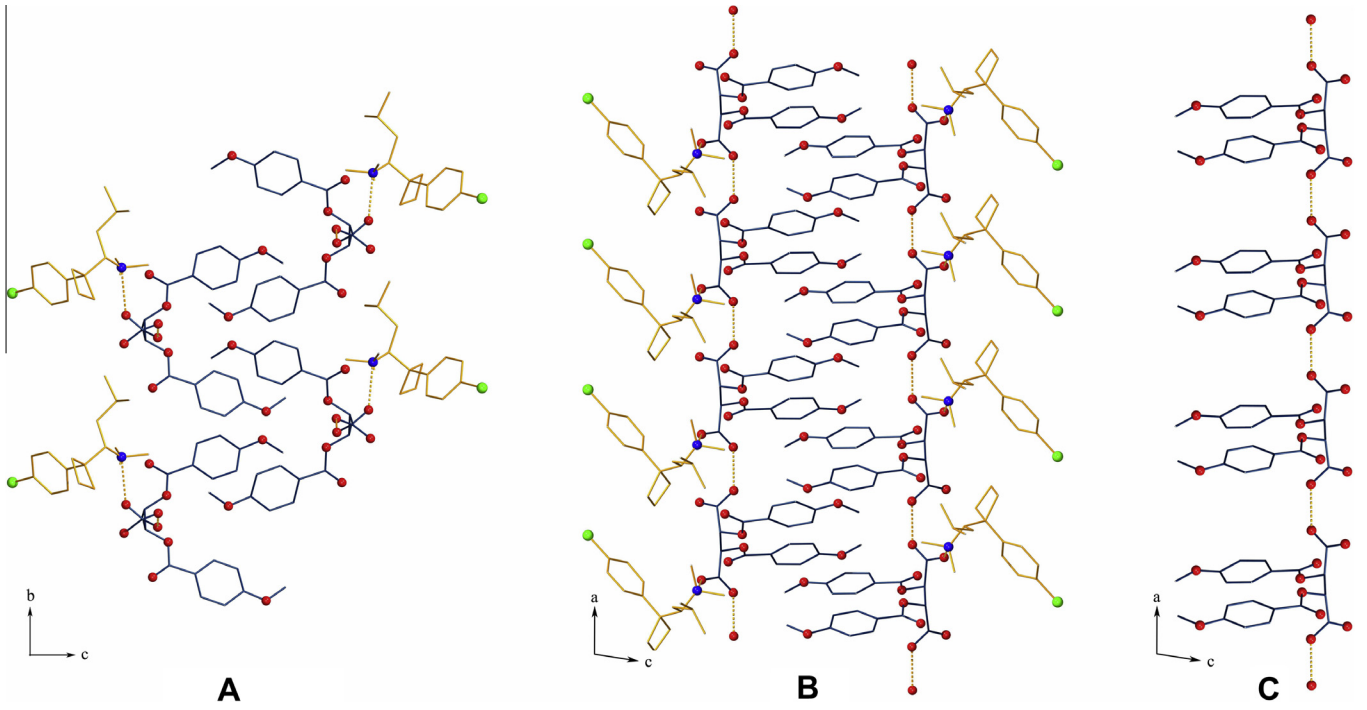

Figure 1. Crystal structures of (*S*)-**1**·(*R*,*R*)-DMTA **5**. Supramolecular ribbon packing structure, (A) top view and (B) side view down the *a* axis; (C) ribbon structure of (*R*,*R*)-DMTA molecules in the more-soluble salt **5**.

Please cite this article in press as: Hu, Y.; et al. *Tetrahedron: Asymmetry* (2015), http://dx.doi.org/10.1016/j.tetasy.2015.04.007

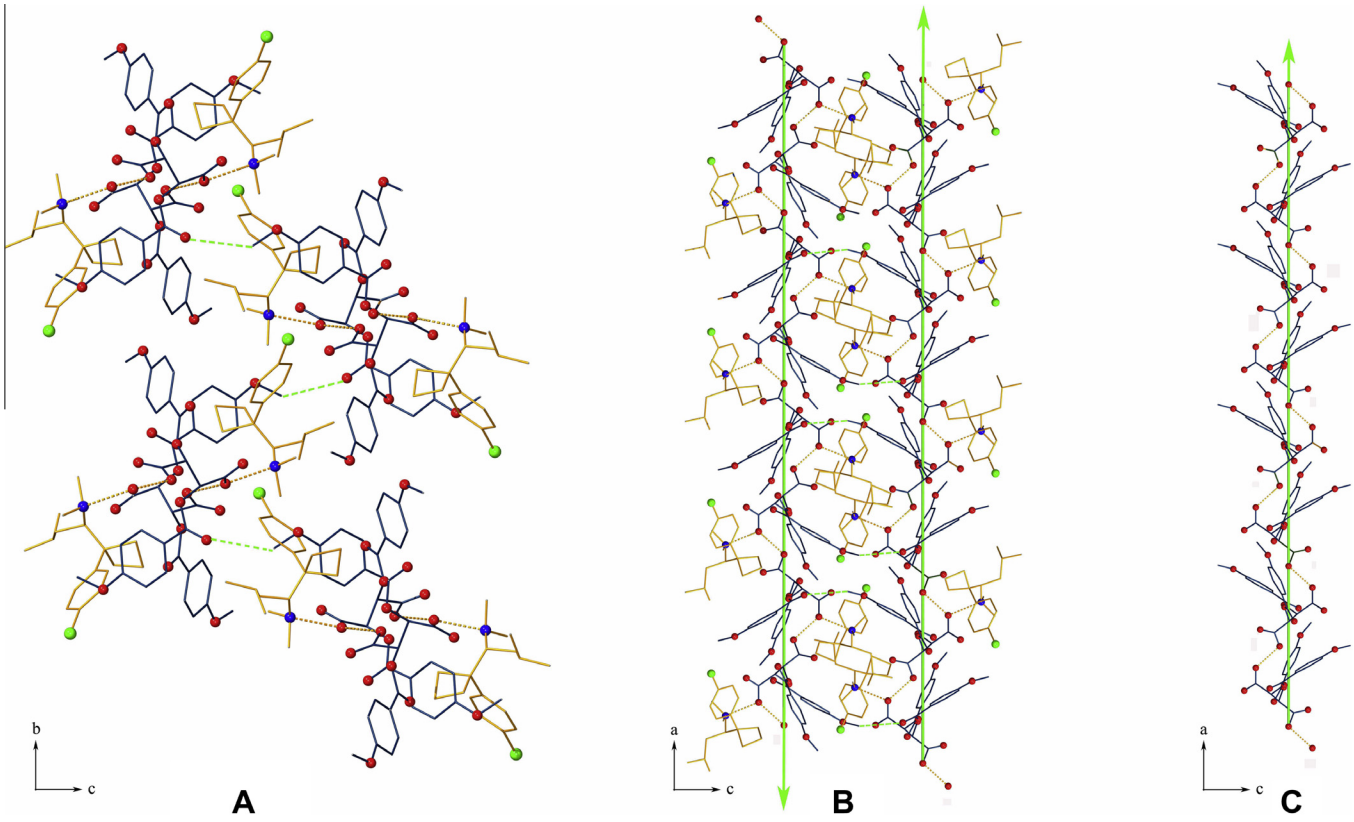

Figure 2. Crystal structures of (*R*)-**1**·(*R*,*R*)-DMTA **6**. Supramolecular spiral net packing structure, (A) top view and (B) side view down the *a* axis; (C) helix structure of (*R*,*R*)-DMTA molecules in the less-soluble salt **6**.

opposite directions. Hence, the substituent groups of tartaric acids are distributed in a staggered formation in the supramolecular construct (Fig. 2B), resulting in a more compact and stable assembly structure. In the less-soluble salt **6**, an additional weak hydrogen bond is formed between the methoxyl group and the carboxylate group of the DMTA molecules of the neighboring helix. It prompts adjacent helices joined together along the vertical direction of helix. Thus, these molecular interactions construct a 'Spiral Mesh' supramolecule. The molecules of sibutramine are embedded in the mesh of the supramolecule and connect to the DMTA molecule chain via salt-bridge hydrogen bonds (Fig. 2A and B).

Compared to the more-soluble salt, the supramolecular structure of less-soluble salt is more compact, with a more precise steric shape complementary between (*R*)-**1** and **4** in the molecular recognition progress. Such factors lead to the difference in properties of diastereomeric salts. For example, melting points of the more-soluble salt (T = 90 °C) and less-soluble salt (T = 161 °C) are significantly different. These differences of diastereomeric salts on the supramolecular structure are good for efficient resolutions.

Interestingly, (*R*)-**1** has been resolved with (*S*,*S*)-DBTA by Fang et al.,[9] while (*R*,*R*)-DMTA was used herein. By the action of hydrogen bonds, tartaric acid framing of DBTA and DMTA all exist as helix motif in the supramolecular structures of less-soluble salts. The helical chains arrange with antiparallel bunches in the crystal (*R*)-**1**·(*R*,*R*)-DMTA **6**, nevertheless, parallel form in the crystal of (*R*)-**1**·(*S*,*S*)-DBTA **7** (Fig. 3). The functional groups of the resolving agents play a characteristic role in diastereomeric salts. In crystal **6**, the methoxy group of DMTA forms additional interactions, for example, weak hydrogen bonding between the methoxyl group and the carboxylate group of another DMTA molecules (Fig. 2A and B). These interactions do not exist in a single crystal of **7**. Hence, the assembly of the supermolecular structures are different, and thus create different chiral structure matching and steric shape complementation. This may be the reason as to why (*R*)-**1** could be obtained by two different configurations tartaric acid derivatives.

In enantiomeric resolution, a pair of diastereomers differ from each other as molecular complexes and preferential crystallization is the result of a more favorable molecular complex formation.[19] Thus, we concluded that the different supramolecular structures of the pair of diastereomeric salts originate from the molecular chiral matching between **4** and the enantiomers of **1**, and contribute to the chiral discrimination of the diastereomeric salts and the effective resolution of *rac*-**1**. The substituent effect has an important impact on the self-assembly characteristic of molecules, structure of the aggregates, and the resolution efficiency in the process of resolution.

3. Conclusion

A facile method for the resolution of sibutramine has been established. An effective resolving agent **4** was found by 'Dutch resolution' from the tartaric acid derivate, and enantiomerically pure (*R*)-**1** was prepared with >98% ee in 84.5% overall yield. The single crystals of the diastereomeric salts were all obtained in ethanol. X-ray crystallographic studies revealed that (*R*)-**1**·(*R*,*R*)-DMTA forms a 'Spiral Mesh' supramolecular structure, while (*S*)-**1**·(*R*,*R*)-DMTA forms a parallel 'zip-closed' ribbon supramolecular structure. Resolving host–guest supramolecular structures are greatly influenced by the functional groups in resolving agents. Compound (*R*)-**1** can be resolved with (*S*,*S*)-DBTA or (*R*,*R*)-DMTA. These different supramolecular structures originate from chiral structure matching and steric shape complementation in the host–guest complex. It is noteworthy that the combination of drugs and receptors in the body is greatly influenced by the different

Please cite this article in press as: Hu, Y.; et al. *Tetrahedron: Asymmetry* (2015), http://dx.doi.org/10.1016/j.tetasy.2015.04.007

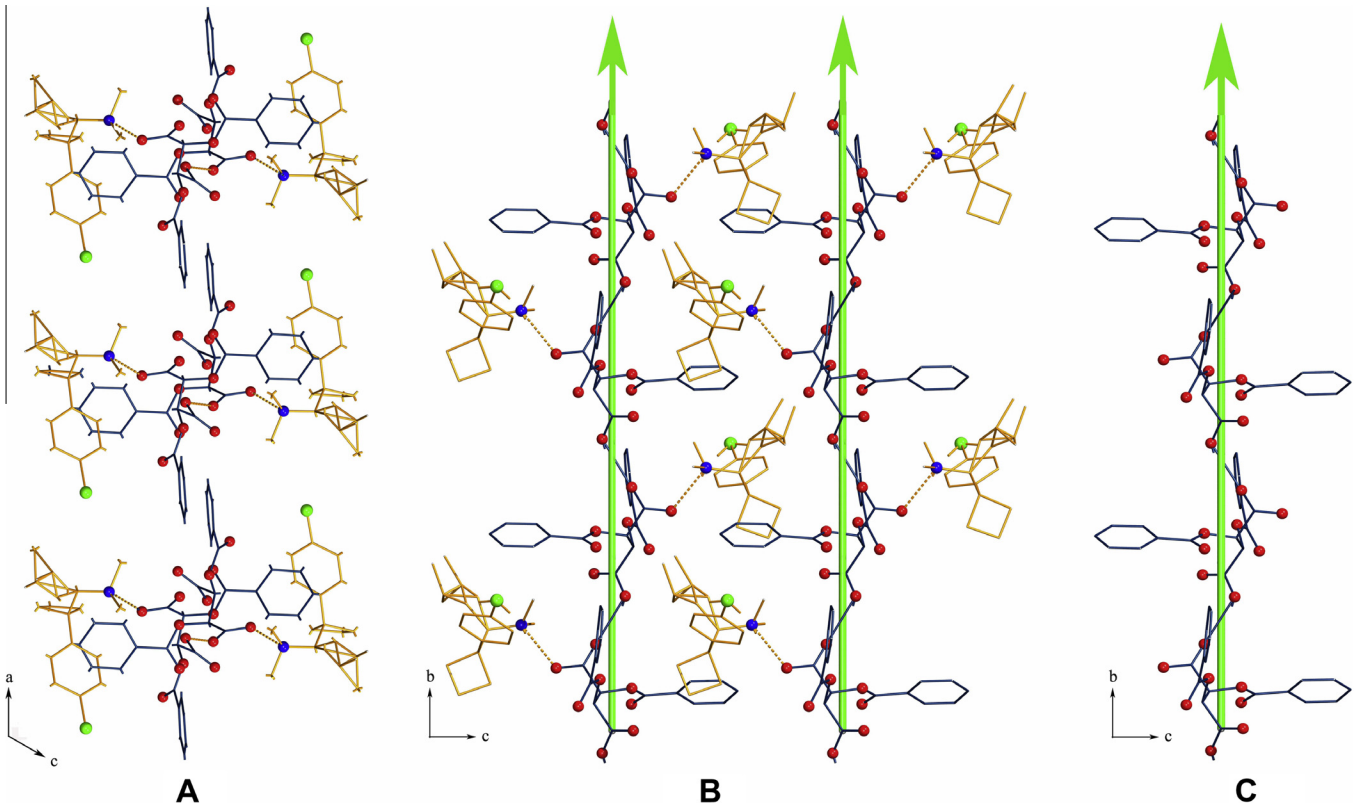

Figure 3. Crystal structures of less-soluble salt from crystal (*R*)-**1**·(*S*,*S*)-DBTA **7**.[9] (A) Top view and (B) side view down the screw axis of DBTA; (C) helix structure of (*S*,*S*)-DBTA molecules.

functional groups and configuration of the drugs. The resolution process is a simple model for recognition, which plays an important role in biological systems and the preferred 'biological answer' is the crystallization of one of the diastereomeric salts.

4. Experimental

4.1. General

Racemic sibutramine hydrochloride was obtained from commercial resource and was used without further purification. The resolving agents (*R*,*R*)-DBTA **3**, (*R*,*R*)-DTTA **4**, (*R*,*R*)-DMTA **5,** and (*S*,*S*)-DMTA were commercially available or made in our laboratory.[20] All solvents were purified by standard procedures. All chemicals were analytically pure. ^{1}H NMR and ^{13}C NMR spectra were taken on a 400 MHz spectrometer. Chemical shifts of ^{1}H NMR are expressed in ppm with the residual signal of $CDCl_3$ as an internal standard (δ = 7.26 ppm). Melting points were obtained on a digital melting point apparatus and are uncorrected. IR spectra were measured on a Nicolet MX-1 spectrometer by the KBr method. Optical rotations of chiral compounds were measured on Perkin–Elmer 341 automatic polarimeter. The enantiomeric excess values of **1** were determined by HPLC analyses using an Agilent-1100 instrument equipped with Chiralpak OD-H column (4.6 × 250 mm). The mobile phase was hexane/isopropanol (90:10) with 0.05% trifluoroacetic acid and flow rate was 1.0 mL/min under detection wavelength of 222 nm. Retention time: (*R*)-**1** 7.0 min, (*S*)-**1** 12.8 min.

4.2. Resolution of 1

The hydrochloride of sibutramine (47.3 g, 0.15 mol) was dissolved in a solution of Na_2CO_3 (20 g, 0.19 mol) and then extracted with ethyl acetate (300 mL × 4). The organic layer was combined and washed with water (300 mL × 2). The organic phase was dried over anhydrous Na_2SO_4. After the solvent was removed, the free base of sibutramine (41.6 g, 99.4% yield) was obtained as a solid. Mp: 53 °C; ^{1}H NMR (400 MHz, $CDCl_3$, δ): 7.22 (d, *J* = 8.4 Hz, 2H), 7.14 (d, *J* = 8.4 Hz, 2H), 2.89 (dd, *J* = 2.3, 10.8 Hz, 1H), 2.47–2.40 (m, 1H), 2.33–2.26 (m, 1H), 2.16 (s, 6H), 2.12–2.05 (m, 1H), 1.97–1.87 (m, 1H), 1.80–1.71 (m, 1H), 1.56–1.48 (m, 1H), 1.26–1.02 (m, 3H), 0.96 (d, *J* = 6.5 Hz, 3H), 0.87 (d, *J* = 6.5 Hz, 3H) ppm.

Sibutramine **1** (31.0 g, 0.11 mol) was added to a solution of **4** (41.7 g, 0.1 mol) in ethanol (530 mL). While stirring, *n*-hexane (500 mL) was added to the solution. The mixture was heated at reflux for 1 h and then cooled to room temperature. The resulting colorless crystals were collected by filtration and recrystallized in isopropanol. 32.6 g (84.5% yield and 98.6% ee) of the salt of (*R*)-**1**·**4** was obtained. Mp: 161 °C; IR (KBr): ν = 3431, 2955, 2879, 2847, 2040, 1919, 1716, 1614, 1506, 1347, 1252, 1176, 1099, 1024, 846, 769, 699 and 521 cm^{-1}; ^{1}H NMR (400 MHz, $CDCl_3$, δ): 8.03 (d, *J* = 8.8 Hz, 4H), 7.35 (d, *J* = 8.4 Hz, 2H), 7.26 (d, *J* = 8.4 Hz, 2H), 6.83 (d, *J* = 8.8 Hz, 4H), 5.92 (s, 2H), 3.82 (s, 6H), 3.48–3.45 (m, 1H), 2.58–2.19 (m, 10H), 1.74–1.69 (m, 2H), 1.63–1.58 (m, 1H), 1.44–1.36 (m, 1H), 1.28–1.22 (m, 1H), 1.01–0.96 (m, 6H) ppm; ^{13}C NMR (100 MHz, $CDCl_3$, δ): 169.4, 164.3, 162.4, 138.7, 132.4, 131.1, 128.9, 127.7, 121.3, 112.5, 70.8, 70.5, 54.4, 48.3, 34.3, 33.6, 32.5, 24.5, 22.0, 20.9, 14.8 ppm.

4.3. Preparation of salt (*S*)-1·4

(*S*)-**1**·(*S*,*S*)-DMTA (81.8% yield) was obtained from **1** and (*S*,*S*)-DMTA by using the above mentioned method. The colorless solid (6.97 g, 0.01 mol) was stirred in a solution of Na_2CO_3 (1.6 g, 0.015 mol) and then extracted with ethyl acetate (100 mL × 3). The extracts were washed with water (100 mL × 2), dried over

(anhydrous Na_2SO_4), and evaporated. The residue (*S*)-**1** (2.68 g, 96.1% yield and 99.1% ee) was obtained as a colorless solid. Equimolar quantities of (*S*)-**1** and **4** were dissolve in ethyl acetate. After the organic phases concentrated in vacuum, the resulting crystals were collected by filtration. Mp: 90 °C; IR (KBr): ν = 3431, 2961, 2872, 2834, 2730, 2024, 1913, 1722, 1608, 1512, 1468, 1405, 1265, 1170, 1106, 1024, 839, 769, 693 and 515 cm^{-1}; ^1H NMR (400 MHz, $CDCl_3$, δ): 8.02 (d, J = 8.8 Hz, 4H), 7.34 (d, J = 8.4 Hz, 2H), 7.16 (d, J = 8.4 Hz, 2H), 6.83 (d, J = 8.8 Hz, 4H), 5.91 (s, 2H), 3.82 (s, 6H), 3.47–3.45 (m, 1H), 2.69–2.14 (m, 10H), 1.84–1.80 (m, 1H), 1.75–1.65 (m, 2H), 1.43–1.35 (m, 1H), 1.28–1.20 (m, 1H), 1.00–0.96 (m, 6H) ppm; ^{13}C NMR (100 MHz, $CDCl_3$, δ): 169.4, 164.3, 162.4, 138.6, 132.4, 131.1, 128.9, 127.7, 121.3, 112.5, 70.9, 70.4, 54.4, 48.4, 34.2, 33.6, 32.6, 24.5, 22.1, 20.9, 14.9 ppm.

4.4. Growth of single crystals and crystallographic analysis

Single crystals **5** and **6** were obtained from ethanol. X-ray crystallographic data were collected on a Bruker Smart 1000 CCD diffractometer with graphite monochromatic MoK_α radiation (λ = 0.71073 Å) and the empirical absorption corrections were applied using the SADABS program.[21] All calculations were performed using the SHELXTL-97 system of computer programs.[22] CCDC reference numbers 1048398–1048399.

Acknowledgements

We are grateful for the financial support from the Science Fund of the Technology Office of Jiangxi, China (20133BBE50016) and the Science Fund of the Health Department of Jiangxi, China (20133172).

References

1. Pavlik, V.; Fajfrova, J.; Slovacek, L.; Drahokoupilova, E. *Bratislava Med. J.* **2013**, *114*, 155–157.
2. Noh, K.; Bae, K.; Min, B.; Kim, E.; Kwon, K. I.; Jeong, T.; Kang, W. *Arch. Pharm. Res.* **2010**, *33*, 267–273.
3. Kang, W.; Bae, K.; Noh, K. *J. Pharm. Biomed. Anal.* **2010**, *51*, 264–267.
4. Bodhankar, S. L.; Thakurdesai, P. A.; Singhal, S.; Gaur, V. *Indian J. Physiol. Pharmacol.* **2007**, *51*, 175–178.
5. Glick, S. D.; Haskew, R. E.; Maisonneuve, I. M.; Carlson, J. N.; Jerussi, T. P. *Eur. J. Pharmacol.* **2000**, *397*, 93–102.
6. Yu, P. Z.; Wang, W. F.; Pan, J. H. CN 200,310,122,864, 2004.
7. Cheetham, S. C.; Heal, D. J. US 6,552,087, 2003.
8. Han, Z. X.; Krishnamurthy, D.; Senanayake, C. H. *Org. Process Res. Dev.* **2006**, *10*, 327–333.
9. Fang, Q. K.; Senanayake, C. H.; Han, Z. X.; Morency, C.; Grover, P.; Malone, R. E.; Bulter, H.; Wald, S. A.; Cameron, T. *Tetrahedron: Asymmetry* **1999**, *10*, 4477–4480.
10. Woodward, R. B.; Cava, M. P.; Ollis, W. D.; Hunger, A.; Daeniker, H. U.; Schenker, K. *Tetrahedron* **1963**, *19*, 247–288.
11. Valente, E. J.; Williams-Knight, P. M.; Moore, M. C. *Chirality* **1998**, *10*, 325–337.
12. Pallavicini, M.; Valoti, E.; Villa, L.; Piccolo, O.; Marchetti, F. *Tetrahedron: Asymmetry* **2000**, *11*, 1957–1964.
13. Sun, X. X.; Li, Y. C.; Zhuang, X. X.; Hu, Y. *Adv. Mater. Res.* **2013**, *781–784*, 135–138.
14. Bialonska, A.; Ciunik, Z. *Cryst. Growth Des.* **2015**, *15*, 358–365.
15. Wang, Y. L.; Chen, A. *Crystallization-Based Separation of Enantiomers*; John Wiley: New York, 2013. pp 1663–1682.
16. Báthori, N. B.; Nassimbeni, L. R. *Cryst. Growth Des.* **2012**, *12*, 2501–2507.
17. Jacques, J.; Collet, A.; Wilen, S. H. *Enantiomers, Racemates and Resolution*; John Wiley: New York, 1981. pp 259–260.
18. Dunitz, J. D.; Gavezzotti, A. *Chem. Soc. Rev.* **2009**, *38*, 2622–2633.
19. Faigl, F.; Fogassy, E.; Nógrádi, M.; Pálovics, E.; Schindler, J. *Tetrahedron: Asymmetry* **2008**, *19*, 519–536.
20. Zhou, Z. Z.; Hu, Y.; Sun, X. X.; Guo, Y.; Yao, H.; Chen, H. W. CN 200,810,026,826, 2008.
21. Sheldrick, G. M. *SADABS, Program for Empirical Absorption Correction of Area Detector Data*; University of Göttingen: Göttingen, 1996.
22. Sheldrick, G. M. *SHELXTL-97, Program for Crystal Structure Solution and Refinement*; University of Göttingen: Göttingen, 1997.